Available online at www.sciencedirect.com
ScienceDirect
Tectonophysics xx (2008) xxx–xxx
TECTONOPHYSICS
www.elsevier.com/locate/tecto

Defining the southern margin of Avalonia in the Pontides: Geochronological data from the Late Proterozoic and Ordovician granitoids from NW Turkey

Aral I. Okay [a,*], Erdin Bozkurt [b], Muharrem Satır [c], Erdinç Yiğitbaş [d], Quentin G. Crowley [e,1], Cosmas K. Shang [c]

[a] *İstanbul Teknik Üniversitesi, Avrasya Yerbilimleri Enstitüsü, Maslak TR-34469, İstanbul, Turkey*
[b] *Middle East Technical University, Department of Geological Engineering, TR-06531 Ankara, Turkey*
[c] *Institut für Geowissenschaften, Üniversität Tübingen, Wilhelmstrasse 56, D-72074 Tübingen, Germany*
[d] *Çanakkale Onsekiz Mart Üniversitesi, Jeoloji Mühendisliği Bölümü, TR-1700 Çanakkale, Turkey*
[e] *NERC Isotope Geosciences Laboratory, Kingsley Dunham Centre, Keyworth, Nottingham NG12 5GG, United Kingdom*

Received 30 May 2007; received in revised form 7 February 2008; accepted 13 February 2008

Abstract

We provide new isotopic data from the Pontides, which substantiate the presence of a Cadomian basement with latest Proterozoic granitoids but also show the existence of Ordovician intrusives. Before the opening of the Black Sea, the Pontides formed a Palaeozoic orogenic belt at the margin of the East European Platform (Baltica) in an analogous position to the Variscan terranes in the central Europe. The Pontides consist of three terranes: The Strandja terrane has a Variscan basement with Carboniferous and Permian granitoids and an epicontinental Triassic to Jurassic sedimentary cover. The İstanbul terrane has a Cadomian basement overlain by a sedimentary sequence of Ordovician to Carboniferous age. It underwent contractional deformation during the Late Carboniferous. The Sakarya terrane is characterized by Carboniferous high temperature metamorphism and plutonism. The boundary between the İstanbul and Sakarya terranes forms a complex tectonic zone several tens of kilometres wide. The new age data come from this boundary zone in the Armutlu peninsula in northwest Turkey. Metagranitoids, which intrude amphibolites in the Armutlu peninsula, give latest Proterozoic and Ordovician U–Pb zircon laser ablation MC–ICP–MS and Pb–Pb evaporation ages. The latest Proterozoic (ca. 570 Ma) granitoids are similar in age to those reported previously from the basement of the İstanbul terrane; they all form part of the widespread Pan-African granitoid plutonism on the margins of Gondwana. The Mid to Late Ordovician granitoids (460 Ma), on the other hand, probably have formed during the rifting of the İstanbul terrane away from Gondwana during the opening of the Rheic ocean. In terms of the tectonic position, stratigraphy and geological evolution, the İstanbul and Sakarya terranes are comparable to the Avalonia and the Armorican terrane assemblage in central Europe, respectively.

Keywords: Pontides; Cadomian; Ordovician granitoid; Variscan; İstanbul terrane; Zircon dating

1. Introduction

The central Europe is made up of a number of Variscan continental blocks squeezed between the two former continents of Baltica and Gondwana (Fig. 1). The microcontinents are generally assigned to an Avalonian block in the north separated by a Rheic suture from an Armorican terrane assemblage in the south; the latter consists of several smaller continental blocks separated by minor oceans (e.g., Franke, 2000; Matte, 2001). The Avalonia is believed to have been detached from the margins of the Gondwana during the Early Ordovician (Arenig) with the opening of Rheic ocean to its south and eventually collided with Baltica during the latest Ordovician (Ashgill) (e.g., Cocks and Torsvik, 2002).

The Avalonian Block and the Rheic suture can be traced from the southwest England into central and north Germany and

* Corresponding author. Tel.: +90 212 285 6208.
E-mail addresses: okay@itu.edu.tr (A.I. Okay), erdin@metu.edu.tr (E. Bozkurt), satir@uni-tuebingen.de (M. Satır), eyigitbas@comu.edu.tr (E. Yiğitbaş), qcrowley@bgs.ac.uk (Q.G. Crowley), cosmas@uni-tuebingen.de (C.K. Shang).
[1] Tel.: +44 115 9363278.

0040-1951/$ - see front matter © 2008 Elsevier B.V. All rights reserved.
doi:10.1016/j.tecto.2008.02.004

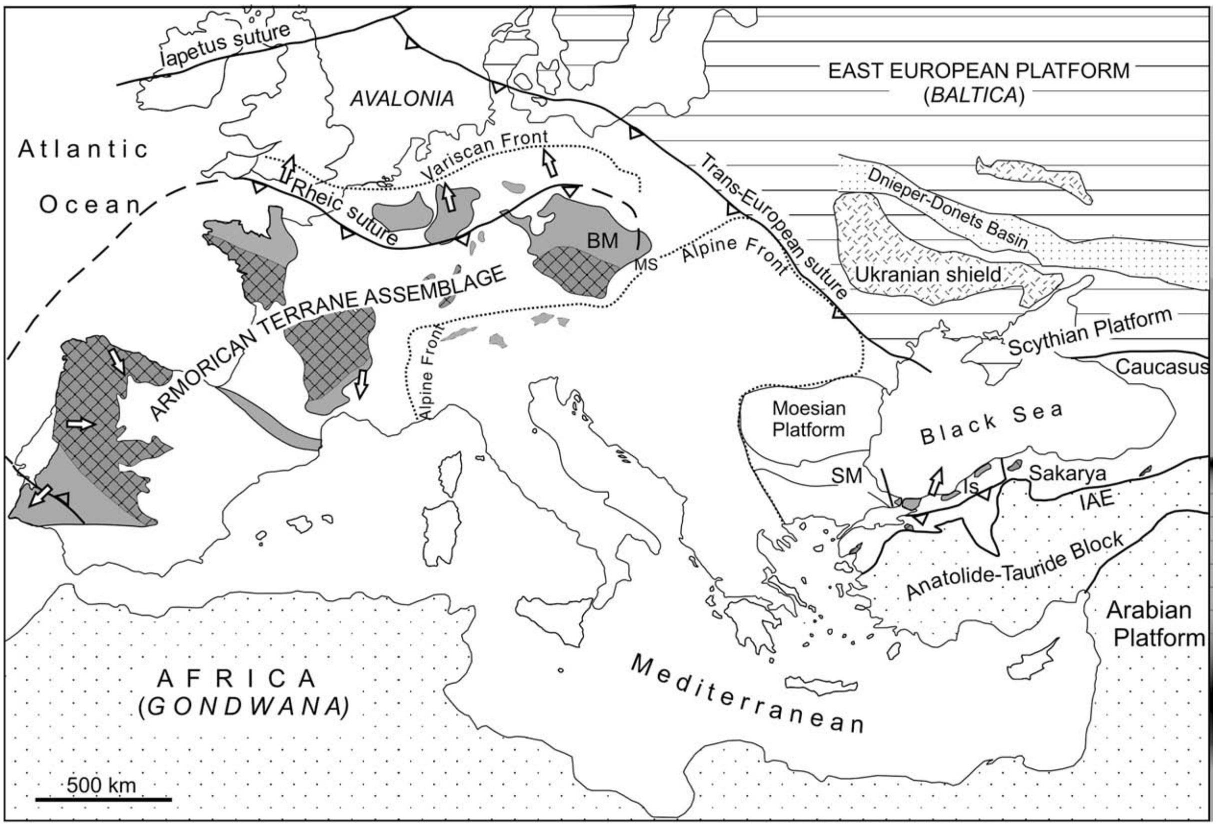

Fig. 1. Simplified tectonic map of Europe showing the major Variscan units. The hachured pattern indicates regions with medium to high grade Carboniferous metamorphism. The triangles on the sutures indicate subduction polarities and the arrows the vergence of Variscan deformation. BM, Bohemian Massif; MS, Moravo–Silesia; Is, İstanbul terrane; IAE, Izmir–Ankara–Erzincan suture; SM, Strandja Massif.

across western Poland into the Moravo–Silesian region (e.g., Pharaoh, 1999; Winchester and The PACE TMR Network Team, 2002; Linnemann et al., 2007). They cannot be followed farther east because of the Mesozoic–Tertiary cover and because of the masking effects of the Alpide orogeny. The southwestern margin of the Baltica (East European Platform), on the other hand, can be followed from the North Sea down to the Black Sea as the Trans-European suture zone (Fig. 1). Before the Cretaceous opening of the oceanic Black Sea basin, the Pontides of northern Turkey were adjacent to the East European Platform, in a tectonic position analogous to the Variscan terranes in Central Europe. They therefore constitute a link between the Variscan chain and the Caucasus–Ural mountains, all forming a rim of Palaeozoic orogens around the Baltica (e.g., Nikishin et al., 1996). In this paper we explore the relation and possible correlation of the Pontides with the Variscan terranes in the light of new isotopic data from the crystalline Pontic basement.

2. Geological setting

The Pontides constitute the Alpide mountain chain north of the Tethyan İzmir–Ankara–Erzincan suture (Ketin, 1966). They are mildly to moderately shortened by folding and thrusting during the Cretaceous and Tertiary Alpide orogeny, but have not been metamorphosed and retain stratigraphic evidence for older orogenies. In contrast, the Anatolide–Taurides south of the suture have undergone Cretaceous and Tertiary regional metamorphism in the internal (northern) domains, and have been intensely shortened mainly by thrusting in the external (southern) regions. Many stratigraphic sections in the Taurides extend from Cambrian to Cretaceous with no intervening episodes of deformation (Özgül, 1976; Gutnic et al., 1979) indicating that the Anatolide–Tauride platform has not been affected by the Variscan orogeny. There is also no evidence for Carboniferous metamorphism in the Anatolide–Taurides. During the Palaeozoic the Anatolide–Tauride platform constituted part of Gondwana from which it was separated in the Triassic with the opening of the southern branch of the Neo-Tethys (e.g., Garfunkel, 2004).

The Pontides are made up of three terranes, each with a distinctive stratigraphy and geological evolution (Fig. 2). The geological features of these terranes are summarized below.

2.1. The Strandja Massif

The Strandja Massif forms part of the large crystalline terrane in the southern Balkans, which also includes the Rhodope and Serbo-Macedonian massifs. It consists of a crystalline basement overlain by a Triassic–Jurassic epicontinental sedimentary sequence (Fig. 3). The basement is made up of predominantly quartzo-feldispathic gneisses intruded by Early Permian (257±6 Ma) granitoids (Aydın, 1988; Okay et al., 2001; Sunal et al., 2006). Zircon Pb–Pb dating has shown

Please cite this article as: Okay, A.I., et al., Defining the southern margin of Avalonia in the Pontides: Geochronological data from the Late Proterozoic and Ordovician granitoids from NW Turkey, Tectonophysics (2008), doi:10.1016/j.tecto.2008.02.004

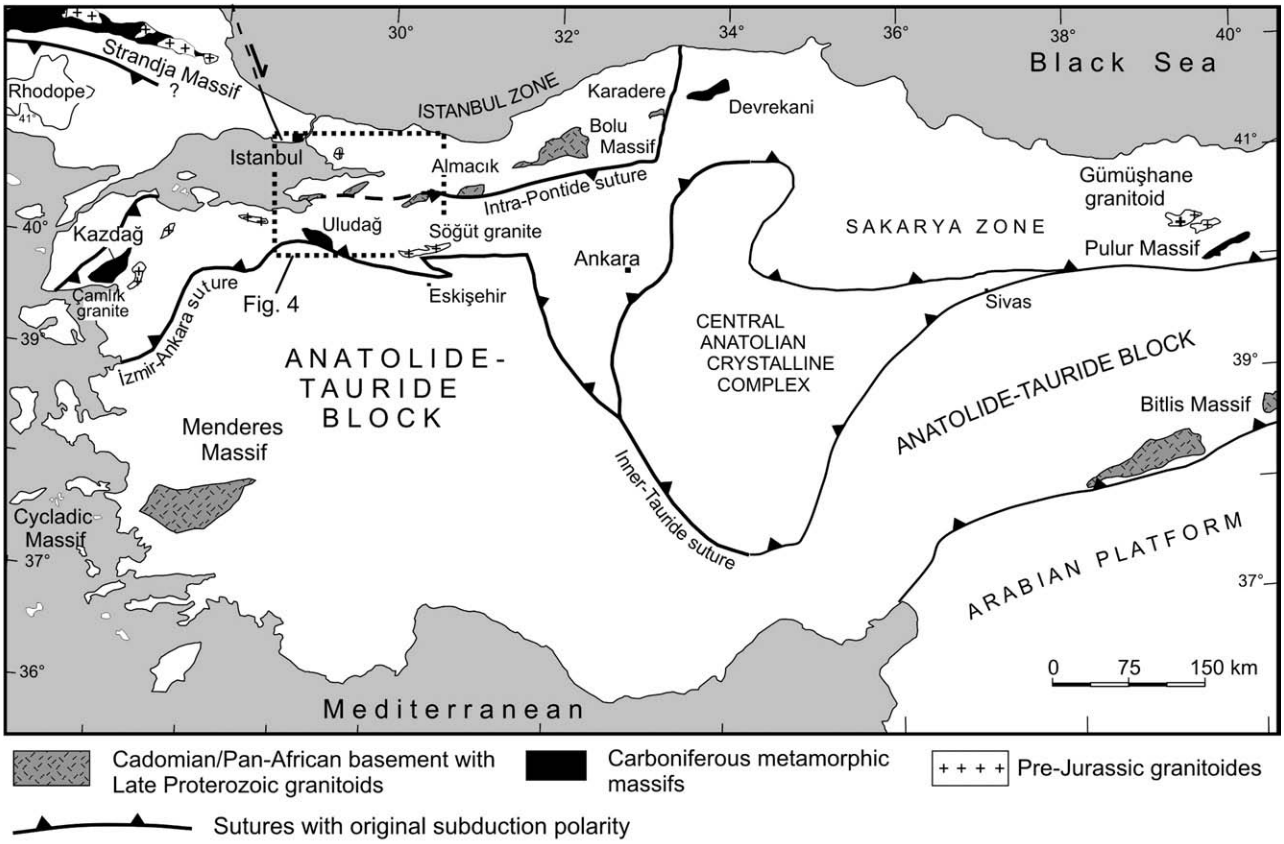

Fig. 2. Tectonic map of western Turkey with the outcrops of the crystalline basement.

that some of the orthogneisses in the basement have intrusion ages of ~313 Ma. This indicates a period of deformation and metamorphism during the Late Carboniferous or Early Permian.

A sedimentary sequence of Triassic and Jurassic age lies unconformably on the Variscan basement (Chatalov, 1988). The Triassic series resemble the Germanic Triassic facies with a thick sequence of Lower Triassic continental clastic rocks overlain my middle Triassic shallow marine carbonates (Fig. 3). At around the Jurassic–Cretaceous boundary (150–155 Ma) the Strandja Massif underwent a second phase of deformation and metamorphism involving north to northeast vergent thrusting (Okay et al., 2001). The deformation was associated with emplacement of Triassic allochthons. The metamorphic rocks are unconformably overlain by mid Cretaceous (Cenomanian) shallow marine sandstones.

2.2. The İstanbul terrane

The İstanbul terrane is a continental fragment, 400 km long and 55 km wide (onshore part), on the southwestern margin of the Black Sea. It is characterized by a continuous and well-developed sedimentary succession ranging from Ordovician to Carboniferous (e.g., Haas, 1968; Görür et al., 1997; Dean et al., 2000) deposited on a Proterozoic metamorphic basement. There are marked stratigraphic differences between the western and eastern parts of the İstanbul terrane (Fig. 3), which led to suggestions that it consists of two different terranes (Kozur and Göncüoğlu, 1998; von Raumer et al., 2002). However, the stratigraphic differences, particularly pronounced in the Carboniferous, can be explained by lateral facies changes (cf. Okay et al., 2006). Furthermore, no Palaeozoic ophiolite has been found in the İstanbul terrane to substantiate its composite character.

The crystalline basement of the İstanbul terrane is commonly divided into four units: (a) A medium to high-grade metamorphic sequence dominated by quartzo-feldspathic gneiss and amphibolite, which constitutes the structurally lowest tectonic unit, (b) a disrupted metaophiolite, which is best exposed in the Almacık Massif where amphibolites are interbanded with layers of metaperidotite and metagabbro (Yılmaz et al., 1981; Yiğitbaş et al., 2004). (c) a sequence of low-grade metavolcanic (meta-andesites with minor metarhyolites) and metasedimentary rocks, with a geochemistry compatible with a subduction-related tectonic setting (Ustaömer and Rogers, 1999; Yiğitbaş et al., 2004), (c) voluminous intrusive granitoids (Yiğitbaş et al., 1999; Ustaömer and Rogers, 1999; Yiğitbaş et al., 2004).

The first three metamorphic units exhibit mutual tectonic contacts and are extensively intruded by granitoidic plutons. The plutons, which make up more than half of the Bolu Massif, are calc-alkaline, tonalite to granodiorite in composition, and their geochemistry is in line with a subduction-related origin. Zircon ages of two plutons from the Bolu Massif are 565 ± 2 and 576 ± 6 Ma (Ustaömer et al., 2005). Similar arc-related granitoids are exposed in the Karadere in the easternmost part of the İstanbul terrane (Fig. 2). They yielded zircons ages between 590 and 560 Ma (Chen et al., 2002) similar to those

Please cite this article as: Okay, A.I., et al., Defining the southern margin of Avalonia in the Pontides: Geochronological data from the Late Proterozoic and Ordovician granitoids from NW Turkey, Tectonophysics (2008), doi:10.1016/j.tecto.2008.02.004

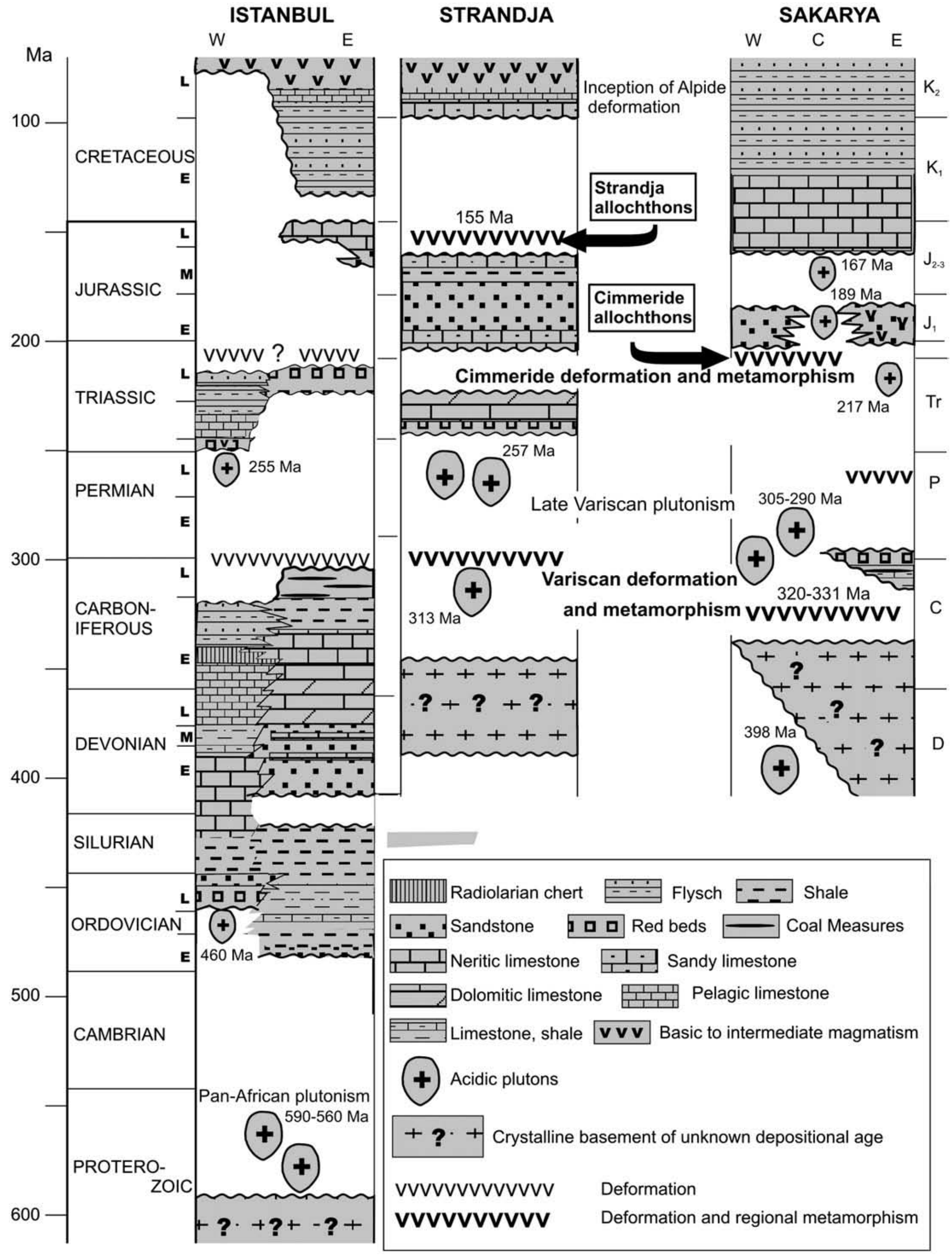

Fig. 3. Stratigraphic columns of the Pontide terranes showing the major plutonic and metamorphic events (modified from Okay et al., 2006).

from the Bolu Massif. Their Sr and Nd isotope values are consistent with formation in a continental arc setting. The Rb/Sr biotite ages from the Karadere basement are 548–545 Ma showing that the basement was not heated above 300 °C since the latest Proterozoic (Chen et al., 2002).

In terms of age, lithology and geochemistry, the basement of the İstanbul terrane is similar to the Pan-African basement of the Gondwana margin. Large areas in northern margins of Gondwana are characterized by Late Proterozoic–Cambrian plutonism and metamorphism forming part of the Pan-African/Cadomian orogenic cycle (e.g., Stern, 1994). On the other hand, the Ukrainian Shield, which constitutes the southern part of the East European Platform north of the Black Sea, consists of Archaen-Palaeoproterozoic crystalline rocks, which were consolidated by 2.3–2.1 Ga (e.g., Bogdanova et al., 1996; Claesson et al., 2001). Therefore, the İstanbul terrane is generally regarded as a continental fragment derived from Gondwana (e.g., Stampfli, 2000).

The Palaeozoic sequence of the İstanbul terrane was deformed with north to northeast vergence during the Carboniferous (Zapcı et al., 2003) and was intruded by a Permian (~255 Ma) granitoid (Yılmaz, 1977). Lower Triassic red sandstones and conglomerates lie unconformably over the Palaeozoic rocks.

2.3. The Sakarya terrane

The Sakarya terrane forms an elongate crustal ribbon extending from the Biga Peninsula in the west to the Eastern Pontides in the east. In contrast to the İstanbul terrane, the sedimentary sequence starts with Lower Jurassic sandstones, which rest on a complex basement (e.g., Altıner et al., 1991). The crystalline basement of the Sakarya terrane can be broadly divided into three types:

(1) A high-grade Variscan metamorphic sequence of gneiss, amphibolite, marble and scarce metaperidotite; the metamorphism is in amphibolite to granulite facies and is dated to the Carboniferous (330–310 Ma) by zircon and monazite ages from the Pulur, Kazdağ, Devrekani and Gümüşhane massifs (Topuz et al., 2004; Okay et al., 2006; Nzegge and Satır, 2007; Topuz et al., 2007). This Variscan basement was probably overlain by Upper Carboniferous molasse, which is only preserved in the Pulur region in the easternmost part of the Sakarya Zone (Ketin, 1951; Okay and Leven, 1996).

(2) Palaeozoic granitoids with Devonian, Carboniferous or Permian crystallization ages (Delaloye and Bingöl, 2000; Okay et al., 2002, 2006; Topuz et al., 2007). Small outcrops of these Palaeozoic granitoids are scattered throughout the Sakarya terrane (Fig. 2), and are unconformably overlain by Jurassic and younger sediments.

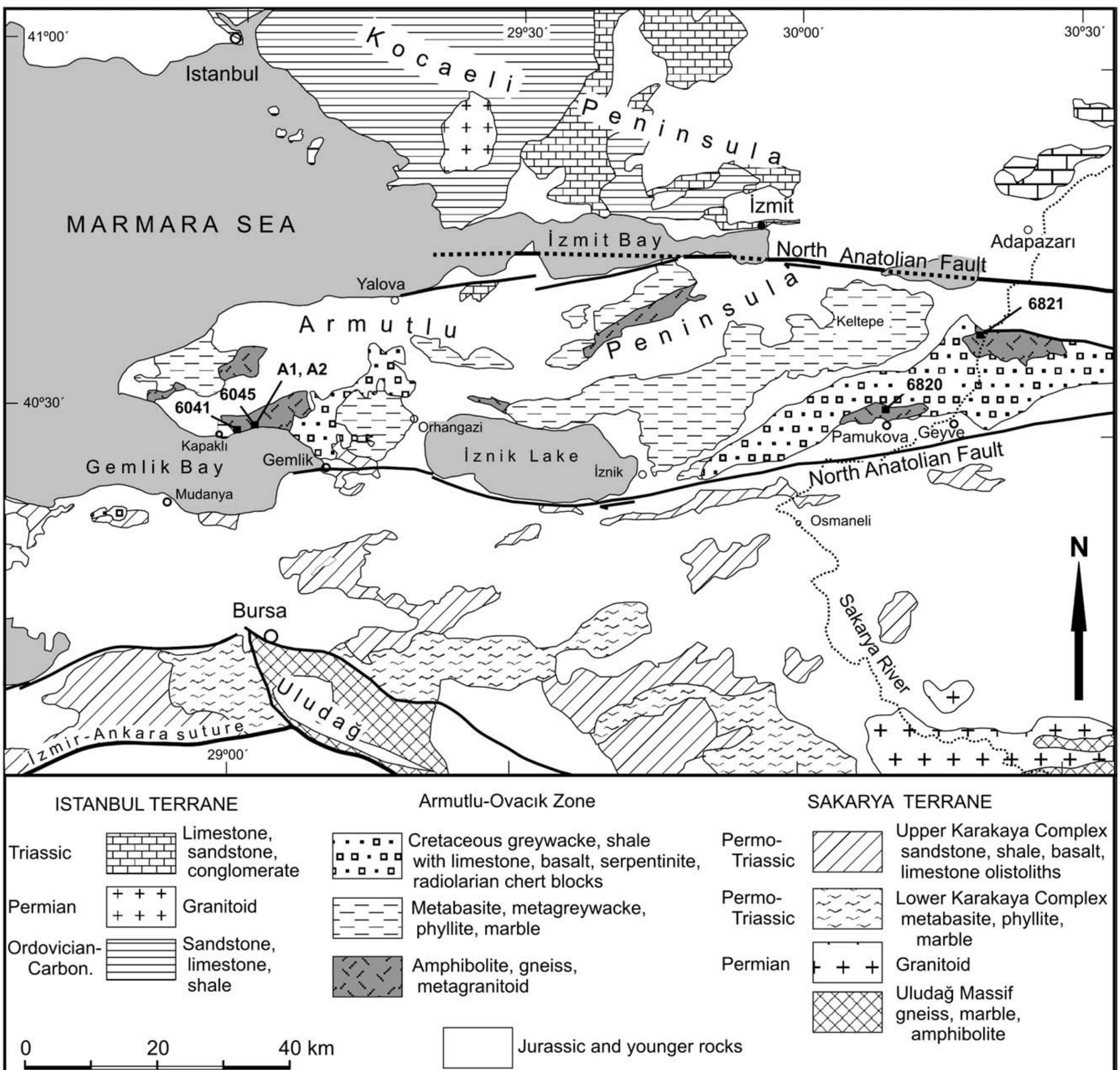

Fig. 4. Geological map of northwest Turkey with the locations of the geochronological samples (based on Türkecan and Yurtsever, 2002; Aksay et al., 2002).

Please cite this article as: Okay, A.I., et al., Defining the southern margin of Avalonia in the Pontides: Geochronological data from the Late Proterozoic and Ordovician granitoids from NW Turkey, Tectonophysics (2008), doi:10.1016/j.tecto.2008.02.004

(3) A low-grade metamorphic complex (the lower Karakaya Complex) dominated by Permo-Triassic metabasite with lesser amounts of marble and phyllite. The Lower Karakaya Complex represents a Permo-Triassic subduction–accretion complex with Late Triassic blueschists and eclogites (Okay and Monié, 1997; Okay et al., 2002), accreted to the margin of Laurussia during the Late Permian to Triassic.

3. The boundary between the İstanbul and Sakarya terranes

The boundary between İstanbul and Sakarya terranes corresponds to a profound stratigraphic, metamorphic and magmatic break, which was denoted by Şengör and Yılmaz (1981) as the Intra-Pontide suture. They envisaged an orthogonal opening between these two terranes in the Liassic and closure during the early Eocene. However, data on the age of the Intra-Pontide ocean are very limited, and even its existence during the Mesozoic is questioned (cf. Elmas and Yiğitbaş, 2001, 2005).

The Kocaeli peninsula in northwest Turkey north of the northern branch of the North Anatolian Fault forms part of the İstanbul terrane (Fig. 4). Conversely the area south of the southern branch of the North Anatolian Fault is unambiguously part of the Sakarya terrane. The region of the Armutlu peninsula bounded by the two branches of the North Anatolian Fault forms a highly complex

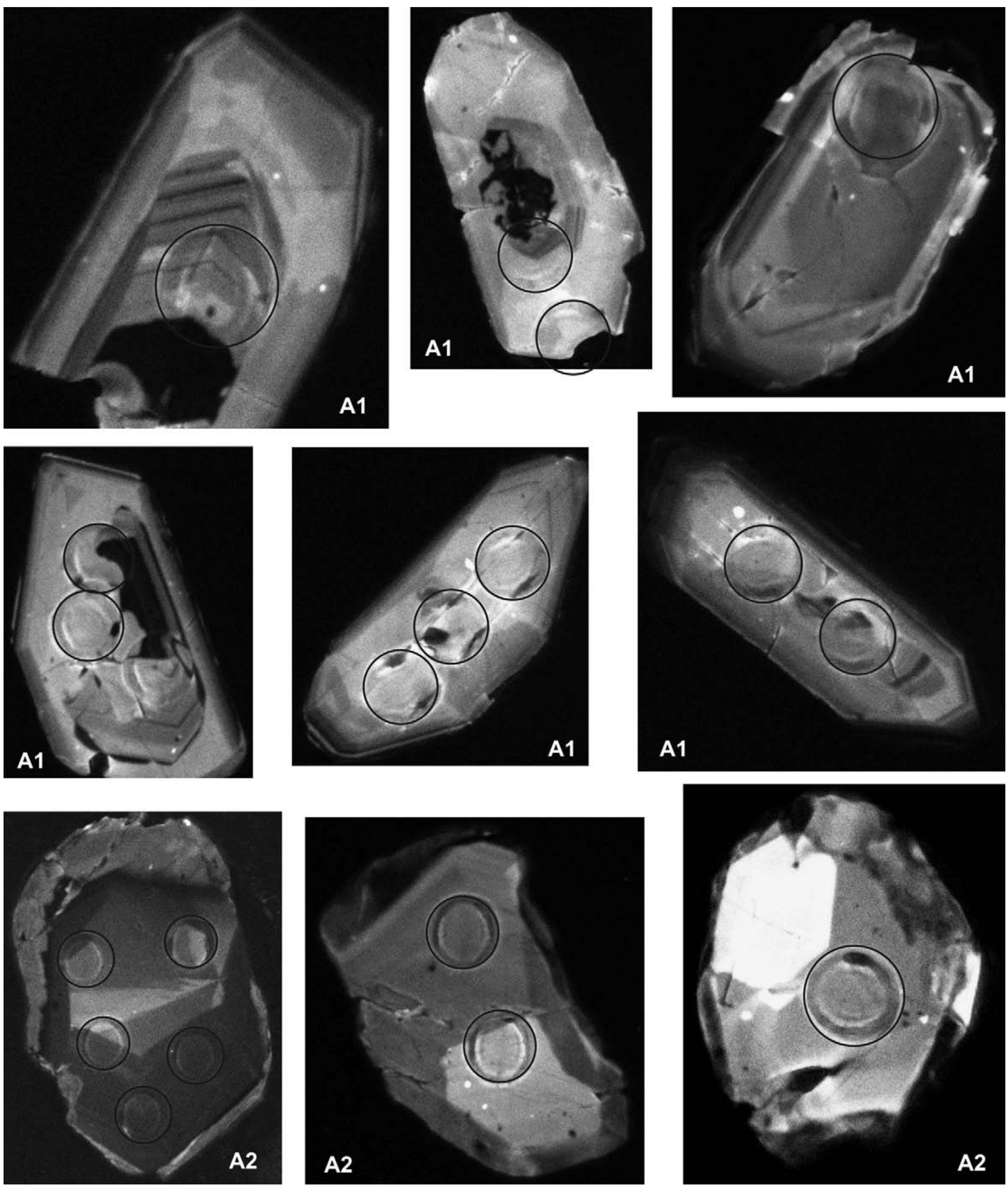

Fig. 5. Cathodoluminiscence images of zircon from the Gemlik area that are dated using laser ablation ICP-MS (samples A1 and A2). The laser ablation pits, marked by circles, are 25 µm in diameter. Most zircon grains show magmatically zoned cores surrounded and locally truncated by fairly homogeneous zircon growths.

tectonic zone, up to 35 km wide, which cannot be easily attributed to either of these terranes (Yılmaz et al., 1995; Yiğitbaş et al., 1999; Elmas and Yiğitbaş, 2001; Robertson and Ustaömer, 2004). This zone, which was called as the Armutlu–Ovacık Zone by Yiğitbaş et al. (1999), is made up of different types of metamorphic rocks and melanges overlain unconformably by Eocene volcanic and sedimentary rocks (Akartuna, 1968; Göncüoğlu and Erendil, 1990). Metamorphic sequences include both a low-grade metavolcanic–metaclastic-carbonate unit and a high-grade sequence of amphibolite and gneiss. A complex geology coupled with scarce biostratigraphic data, lack of isotopic ages and poor exposure resulted in a wide variety of contradictory models for the evolution of the Armutlu Peninsula (e.g., Elmas and Yiğitbaş, 2005; Ustaömer and Robertson, 2005). Here, we present new isotopic data on the high-grade metamorphic rocks from the Armutlu peninsula with the aim of elucidating the tectonic relation between the İstanbul and Sakarya terranes.

4. Isotopic data from the Armutlu Peninsula

Small bodies of gneiss, amphibolite and metagranite form scattered outcrops throughout the Armutlu peninsula (Fig. 4) and generally exhibit tectonic contacts with the surrounding units. They are regarded either as a Cretaceous metamorphosed ophiolite (Yılmaz, 1990; Yılmaz et al., 1995; Aksay et al., 2002) or as the Precambrian basement of the İstanbul terrane (Kaya, 1977; Elmas and Yiğitbaş, 2001; Yiğitbaş et al., 2004). There are no previous isotopic data on their ages. We have dated zircons from the metagranitoids and orthogneisses from the Gemlik, Pamukova and Geyve regions of the Armutlu peninsula using laser-ablation multi-collector inductively coupled mass spectrometry (LA-MC–ICP–MS) and the thermal ionization mass spectrometry (TIMS) Pb–Pb evaporation technique. Details of analytical techniques are given in the appendix. We use the geological time scale of the International Stratigraphic Commission (Gradstein et al., 2004, http://www.stratigraphy.org/gssp.htm).

4.1. Gemlik region

A sequence of banded amphibolites intruded by metagranitoidic veins and stocks crops out along the northern shore of the Gemlik Bay between Gemlik and Kapaklı (Fig. 4, Kaya, 1977; Yiğitbaş et al., 2004). In the east the crystalline rocks are in tectonic contact with a highly deformed and weakly metamorphosed sequence of greywacke, siltstone and shale of the Gemlik Flysch. The Gemlik Flysch comprises rare tectonized olistoliths of limestone, altered basalt, serpentinite and radiolarian chert. Kaya and Kozur (1987) describe latest Jurassic radiolaria from a chert in the Gemlik Flysch indicating a post-Jurassic, most probably Cretaceous age for the unit. In the west the amphibolites and metagranitoids are in contact with slightly metamorphic arkosic sandstones and conglomerates, correlated with the Ordovician clastic rocks of the İstanbul terrane (Kaya, 1977; Yiğitbaş et al., 2004). In the north the high-grade metamorphic rocks are overlain and intruded by a thick sequence of volcanic and hypabyssal rocks of Tertiary age.

The amphibolites in the Gemlik area are massive to banded and consist of hornblende and plagioclase with minor epidote. Repeated attempts to extract zircons from the amphibolites were not successful. The amphibolites are intruded by granitoidic veins and stocks. The granitoidic stocks are up to several hundred metres across. In their margins they comprise xenoliths of amphibolite. They consist dominantly of quartz, feldspar and hornblende; show a weak compositional banding and a low-grade metamorphism. Feldspar grains show evidence for crystal-plastic deformation with undulatory extinction, kinking and deformation bands/lamella and subgrain development, and quartz has recrystallized into subgrains.

We have dated zircons from metagranitoid samples using both LA-MC–ICP–MS (two samples) and TIMS Pb–Pb evaporation (two samples) techniques. Samples A1 and A2 are from coarse-grained granitoid stocks. Sample A1 typically exhibits euhedral

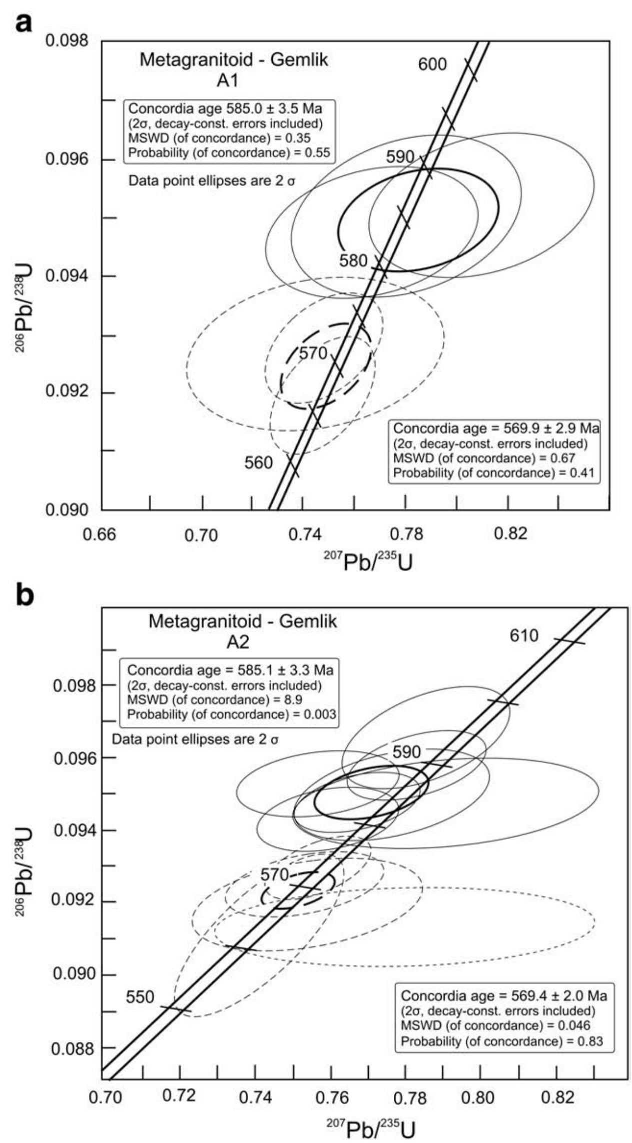

Fig. 6. U–Pb concordia diagrams of zircons from Armutlu peninsula metagranitoids dated using laser ablation ICP-MS. For location of the samples see Fig. 4.

Table 1
U–Pb zircon data from laser ablation multicollector inductively coupled plasma mass spectrometry

Sample	Zircon ID	U ppm	$^{207}Pb/^{206}Pb$	2σ%	$^{207}Pb/^{235}U$	2σ%	$^{206}Pb/^{238}U$	2σ%	Rho [a]	Age (Ma)			% discordance [b]
										$^{207}Pb/^{206}Pb$	$^{206}Pb/^{238}U$	$^{207}Pb/^{235}U$	
A1	Z-2	99.3	0.0583	5.4	0.7449	5.6	0.0927	1.2	0.21	540.8	571.4	565.3	−5.7
	Z-3	132.9	0.0587	4.3	0.7668	4.4	0.0947	1.0	0.22	556.0	583.5	578.0	−4.9
	Z-4	205.9	0.0616	4.3	0.8093	4.4	0.0952	1.1	0.24	661.7	586.3	602.1	11.4
	Z-5	65.4	0.0596	4.5	0.7803	4.6	0.0950	1.2	0.26	587.3	585.2	585.7	0.4
	Z-6	198.0	0.0589	2.0	0.7473	2.1	0.0920	0.9	0.40	564.8	567.1	566.6	−0.4
	Z-7	197.2	0.0585	2.3	0.7481	2.5	0.0928	0.8	0.32	548.5	571.8	567.1	−4.2
A2	Z-1	110.8	0.0594	3.1	0.7535	3.3	0.0919	1.2	0.35	583.3	567.0	570.2	2.8
	Z-2	342.1	0.0594	1.6	0.7580	1.7	0.0925	0.7	0.39	582.0	570.5	572.8	2.0
	Z-4	306.9	0.0590	1.3	0.7565	1.5	0.0929	0.7	0.49	568.4	572.9	572.0	−0.8
	Z-7	485.8	0.0585	1.4	0.7460	1.5	0.0925	0.7	0.47	548.6	570.2	565.9	−3.9
	Z-10	312.8	0.0619	5.2	0.7797	5.3	0.0913	1.0	0.18	671.3	563.4	585.3	16.1
	Z-13	270.2	0.0589	1.6	0.7412	2.6	0.0912	2.1	0.79	565.2	562.5	563.1	0.5
	Z-3	487.1	0.0593	1.7	0.7832	1.9	0.0958	0.8	0.43	578.2	589.7	587.3	−2.0
	Z-5	70.9	0.0587	1.7	0.7670	1.9	0.0948	0.7	0.39	555.8	583.7	578.0	−5.0
	Z-6	221.4	0.0584	1.9	0.7595	2.0	0.0943	0.8	0.37	544.2	581.2	573.7	−6.8
	Z-9	51.2	0.0576	2.2	0.7565	2.4	0.0953	0.8	0.34	513.9	586.7	572.0	−14.2
	Z-11	179.4	0.0593	2.5	0.7763	2.7	0.0950	1.1	0.40	576.8	585.0	583.3	−1.4
	Z-12	74.8	0.0605	4.1	0.7901	4.2	0.0948	1.1	0.25	620.6	583.6	591.2	6.0
	Z-13	252.0	0.0590	2.0	0.7853	2.3	0.0965	1.2	0.51	566.9	594.1	588.5	−4.8

[a] Error correlation coefficient calculated using isoplot (Ludwig, 2003).
[b] Measure of % difference between $^{207}Pb/^{206}Pb$ and $^{206}Pb/^{238}U$ ages.

acicular (ca 150×50×50 μm) to equant (ca 200×150×150 μm) zircon morphologies, whereas those in sample A2 are typically stubby (ca 225×150×150 μ) or equant (ca 125×120×120 μ). CL images of zircons from both A1 and A2 indicate oscillatory zoned "cores" truncated by areas of a fairly homogeneous nature and outermost oscillatory zoned thin "rims", the latter generally less than 10 μ across (Fig. 5). Multiple laser-ablation analyses of zircons gave ages of 585.0±3.5 Ma and 569.9±2.9 Ma for A1, and 585.1±3.3 and 569.4±2.0 Ma for A2 (Fig. 6, Table 1). Although some of the individual analyses for the two separate age populations for both A1 and A2 do overlap within error, it is noteworthy that there is a spatial correlation of the older ca 585 Ma ages only in the inner-most oscillatory zoned portion of the zircons. The younger ca 569 Ma ages were only determined from the fairly homogeneous and outer oscillatory zoned areas of the zircon crystals.

Twelve zircon grains were dated using TIMS Pb–Pb evaporation technique from the sample 6045, which comes from a granitoidic vein in the amphibolites. The zircon grains gave consistent $^{207}Pb/^{206}Pb$ late Proterozoic ages with an average of 569.4±1.4 Ma (Fig. 7a, Table 2). It is noteworthy that TIMS Pb–Pb evaporation and LA-MC–ICP–MS yield a 569.4 Ma age for two different samples. This is also seen as further evidence in support of the two age populations evident in sample A2. The ca 570 Ma age is interpreted as the intrusion age, whereas the ca. 582 Ma age found in both the samples A1 and A2 could represent an older magmatic event. The inferred ca 570 Ma intrusion age of the granitoid and the ca. 582 Ma age of an older magmatic event from the Gemlik area are very similar to those reported from the basement of the İstanbul terrane from the Karadere (Chen et al., 2002) and the Bolu Massif (Ustaömer et al., 2005), which range between 590 and 560 Ma.

The other sample from the Gemlik area (6041) comes from a leucocratic metagranite stock, about 300 m wide, within the amphibolites. Zircon grains from this sample show a distinct igneous growth zoning (Fig. 8). Seven zircon grains from the metagranite stock gave a Middle to Late Ordovician Pb–Pb age of 457±6 Ma, and six grains an Early Ordovician age of 488± 6 Ma (Fig. 7b, Table 2). At different temperature steps some zircon grains (no. 12 and 13) produced ages belonging two both age groups suggesting that the ca. 488 Ma age represents an older magmatic event. In the field the Ordovician metagranite was physically not different from the Late Proterozoic ones, except possibly by its leucocratic character.

4.2. Pamukova region

A sequence of gneiss, micaschist and amphibolite cut by small granitoidic stocks crops out north of Pamukova (Fig. 4, Elmas and Yiğitbaş, 2001). As in the Gemlik area the metamorphic rocks are in tectonic contact with the highly deformed clastic rocks of the Gemlik Flysch. We have dated eight zircons using the TIMS Pb–Pb evaporation technique from a granitoidic body (sample 6820), about 150 m across, intrusive into the amphibolites. The granitoid is leucocratic, medium grained and consists mainly of plagioclase and quartz with minor K-feldspar and chloritized biotite. It has undergone weak metamorphism and cataclasis; quartz has recrystallized into subgrains, whereas plagioclase largely retains its magmatic crystal outlines. Zircons from this sample show crystal outlines and a well-preserved igneous zoning (Fig. 8). They yielded a spread of ages from latest Proterozoic (561 Ma) down to Ordovician (446 Ma) (Fig. 6c, Table 2). The younger ages, which are similar to the 457±6 Ma age from the Gemlik metagranitoid, is interpreted as the age of the intrusion, and the

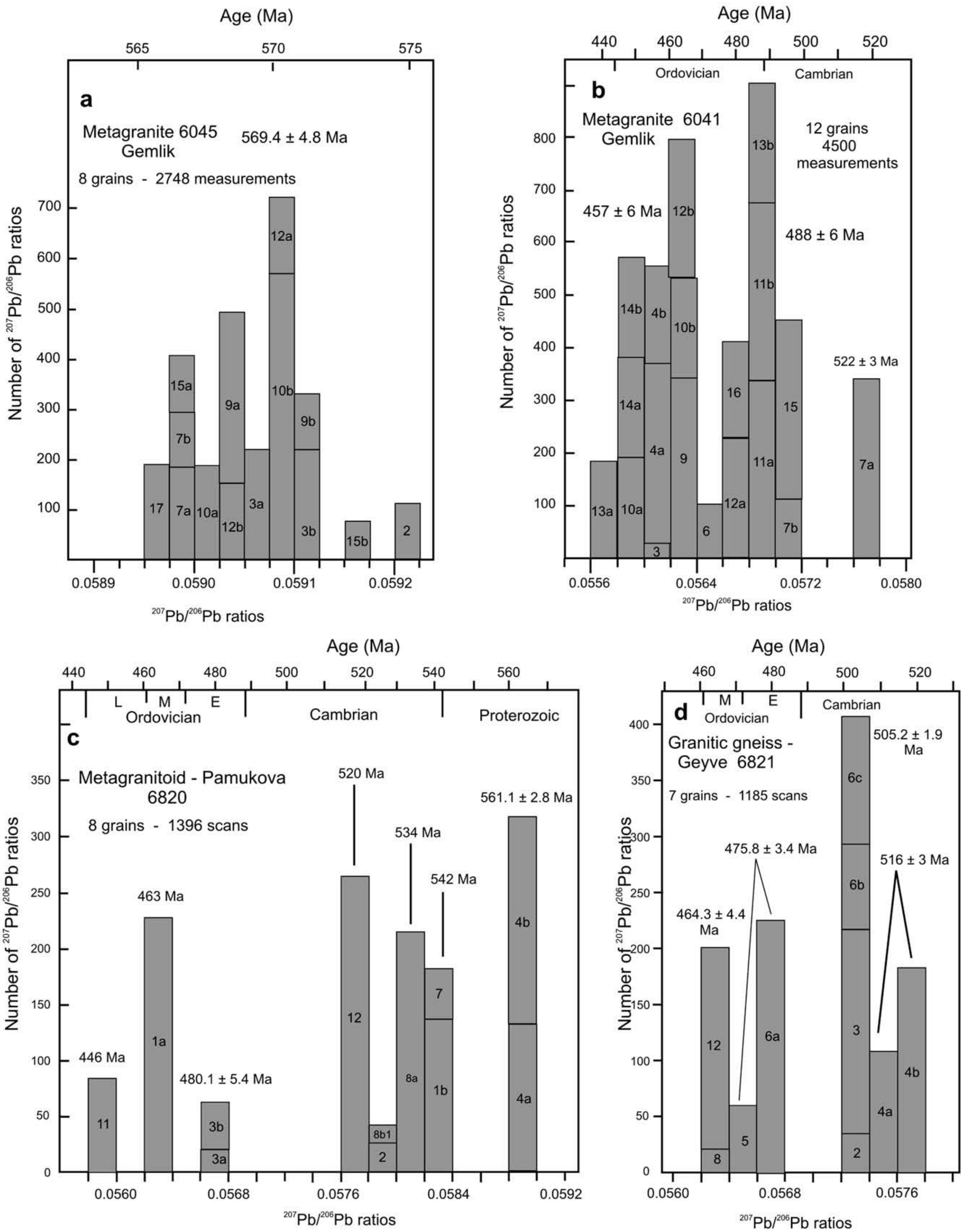

Fig. 7. Histograms showing the distribution of $^{207}Pb/^{206}Pb$ ratios derived from the evaporation of single zircon grains from the Armutlu peninsula. (a) and (b) Gemlik, (c) Pamukova, (d) Geyve areas. For location of the samples see Fig. 4.

Table 2
Isotopic data from single zircon grain Pb/Pb evaporation analyses

Zircon grains	Zircon features	Evap. temp. °C	Number of ratios	$^{204}Pb/^{206}Pb$ ratio	$^{207}Pb/^{206}Pb$ ratio	$^{207}Pb/^{206}Pb$ ages (Ma) and errors
Metagranitoid 6045						
2	125–180 µm, medium, prismatic, yellow	1380	111	0.000034	0.059226±072	575.5±3.6
3	125–180 µm, medium, prismatic, yellow	1400	219	0.000015	0.059058±026	569.3±2.5
		1420	227	0.000015	0.059112±040	571.3±2.7
7	125–180 µm, small, rounded, light-colorless	1380	184	0.00006	0.058988±127	566.7±5.3
		1420	113	0.00003	0.058972±073	566.1±3.5
9	125–180 µm, prismatic, thick, light yellow	1400	342	0.000019	0.059042±030	568.7±2.6
		1420	111	0.000011	0.059114±069	571.3±3.4
10	125–180 µm, prismatic, thick, light yellow	1400	189	0.000016	0.059024±028	568.0±2.5
		1420	569	0.000016	0.059077±038	570.3±2.8
12	125–180 µm, prismatic, thick, light yellow	1400	152	0.000041	0.059079±082	570.0±3.8
		1420	152	0.000032	0.059048±056	568.9±3.1
15	63–125 µm, small, rounded, yellow	1380	113	0.000047	0.058982±074	566.5±3.6
		1400	76	0.000027	0.059152±114	572.7±4.8
17	63–125 µm, thin, rounded yellow	1420	190	0.000084	0.058958±121	565.6±5.1
					mean	569.4±1.4 Ma
Metagranitoid 6041						
3	63–125 µm, tiny, idiomorphic-prismatic, short, light yellow	1380	29	0.000076	0.056190±216	459.9±8.9
4	63–125 µm, big long(>100 µm), xenomorphic, reddish	1380	342	0.000095	0.056056±058	454.6±3.3
		1400	185	0.000083	0.056158±059	458.7±3.3
6	63–125 µm, big long (>100 µm), xenomorphic, reddish	1380	102	0.000811	0.056506±297	472.3±12.1
7	125-200 µm, xenomorphic-irregular crystal faces, brown	1380	340	0.000054	0.057800±040	522.2±2.8
		1400	112	0.000064	0.057160±069	497.8±3.5
9	63–125 µm, small long xenomorphic, brown	1380	341	0.000099	0.056257±068	462.6±3.6
10	63–125 µm, small, idiomorphic-prismatic	1380	190	0.000115	0.055957±033	450.7±2.7
		1400	189	0.00009	0.056352±078	466.3±3.9
11	63–125 µm, small xenomorphic, fragments	1380	337	0.000096	0.056806±060	484.1±3.3
		1400	336	0.000088	0.056899±059	487.6±3.2
12	63–125 µm, small xenomorphic, fragments	1380	226	0.000086	0.056725±074	480.9±3.7
		1400	262	0.000087	0.056255±079	462.5±3.9
13	63–125 µm, xenomorphic, brown	1380	184	0.00013	0.055661±097	438.9±4.5
		1400	228	0.00009	0.056987±049	491.1±3.0
14	63–125 µm, small, xenomorphic, brown	1380	190	0.00009	0.055963±029	450.9±2.6
		1400	190	0.000097	0.055968±055	451.1±3.2
15	63–125 µm, tiny, idiomorphic-fragments	1380	340	0.00008	0.057057±063	493.8±3.4
16	63–125 µm, small, idiomorphic-prismatic, light brown	1380	187	0.000091	0.056742±058	481.5±3.2
		1400	190	0.000098	0.056502±078	472.2±3.8
Metagranitoid 6820						
1	63–125 µm, medium, prismatic, yellow	1380	227	0.000166	0.056275±089	463.3±4.2
		1420	136	0.000077	0.058305±102	541.3±4.5
2	63–125 µm, medium, prismatic, yellow	1390	26	0.000154	0.057962±267	528.4±10.5
3	63–125 µm, big, long idio-prismatic, yellow	1400	20	0.00011	0.056692±225	479.6±9.1
		1420	42	0.00011	0.056713±160	480.4±6.7
4	63–125 µm, big, idio-prismatic, yellow	1400	131	0.000162	0.058853±090	561.7±4.1
		1430	185	0.000141	0.058819±083	560.5±3.9
7	63–125 µm, medium, prismatic, yellow	1400	45	0.012064	0.058363±107	543.5±4.6
8	63–125 µm, medium, prismatic, yellow	1400	214	0.000087	0.058123±091	534.4±4.2
		1420	16	0.011839	0.057909±194	526.3±7.7
		1420	6		0.059406±241	582.0±9.1
11	63–125 µm, medium, prismatic, yellow	1400	84	0.000128	0.055839±074	446.0±3.8
12	63–125 µm, medium, prismatic, yellow	1400	264	0.000183	0.057748±071	520.2±3.6
Granitoidic gneiss 6821						
2	63–125 µm, small, xenomorphic, yellow	1420	35	0.000102	0.057238±197	500.7±8.0
3	63–125 µm, small, xenomorphic, yellow	1420	182	0.000068	0.057388±092	506.5±4.2
4	63–125 µm, small, xenomorphic, yellow	1400	108	0.000056	0.057568±118	513.4±5.1
		1420	183	0.000063	0.057669±075	517.3±3.7
5	63–125 µm, small, xenomorphic, yellow	1420	60	0.000111	0.056587±193	475.5±8.0
6	63–125 µm, small, xenomorphic, yellow	1380	226	0.000095	0.056596±074	475.9±3.7
		1400	76	0.000034	0.057337±040	504.6±2.8
		1420	114	0.000041	0.057373±064	505.9±3.4
8	63–125 µm, small, xenomorphic, yellow	1400	21	0.000133	0.056287±215	463.7±8.5
12	63–125 µm, small, xenomorphic, yellow	1400	180	0.000078	0.056306±078	464.5±4.8

Please cite this article as: Okay, A.I., et al., Defining the southern margin of Avalonia in the Pontides: Geochronological data from the Late Proterozoic and Ordovician granitoids from NW Turkey, Tectonophysics (2008), doi:10.1016/j.tecto.2008.02.004

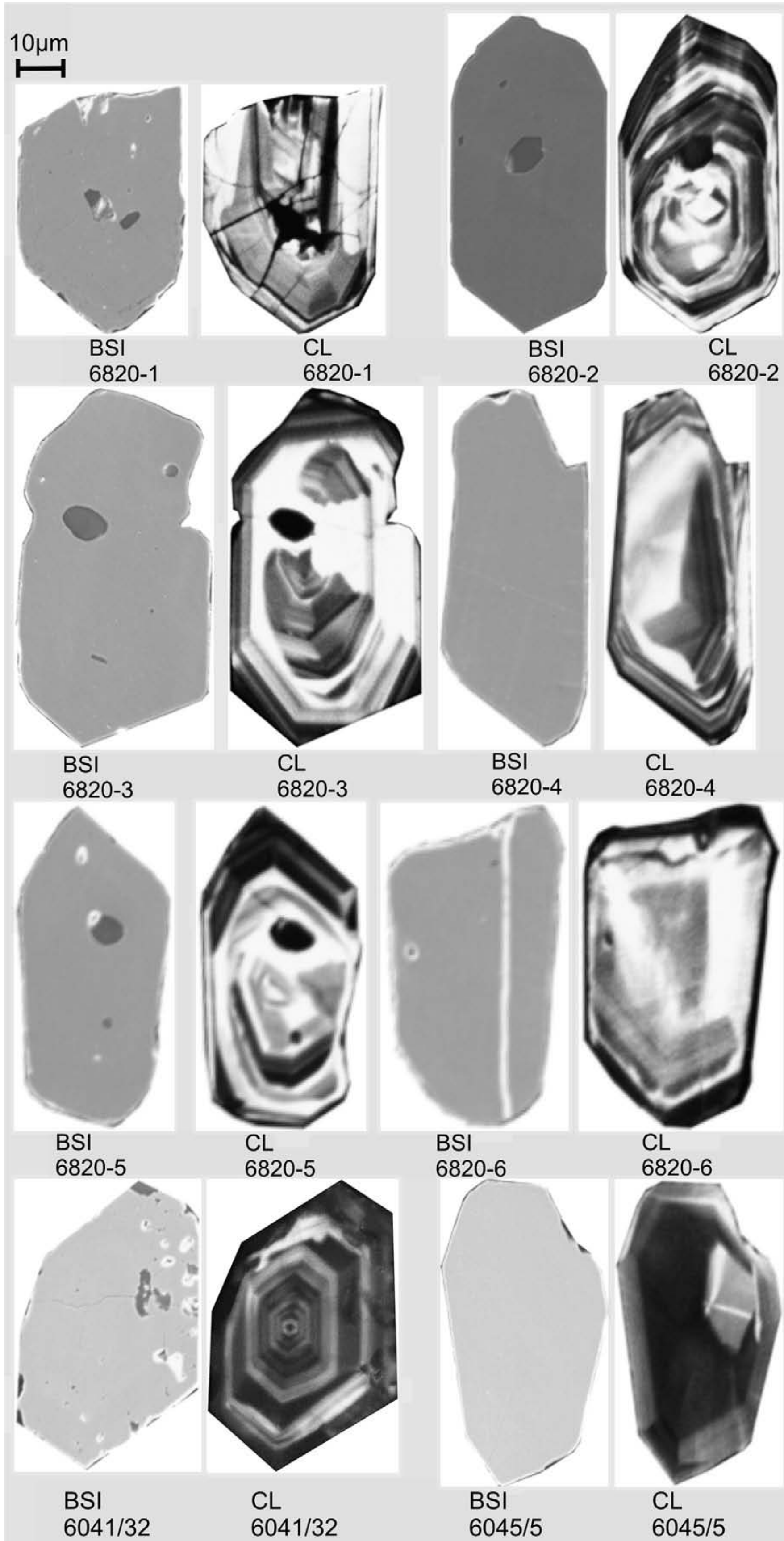

Fig. 8. Backscattered electron (BSI) and cathodoluminiscence (CL) images of representative zircons from Armutlu samples. Zircons from these samples were dated by TIMS Pb–Pb evaporation technique. Most show crystal outline and internal structure marked by oscillatory zoning of magmatic origin.

Please cite this article as: Okay, A.I., et al., Defining the southern margin of Avalonia in the Pontides: Geochronological data from the Late Proterozoic and Ordovician granitoids from NW Turkey, Tectonophysics (2008), doi:10.1016/j.tecto.2008.02.004

older ages are inherited or mixed ages. The 561.1±2.8 Ma age from one zircon grain is, within error limits, the same as the latest Proterozoic age obtained from the Gemlik area.

4.3. Geyve region

Gneiss, amphibolites and metaperidotite crop out in the northern margin of the Geyve gorge along the Sakarya river in tectonic contact with the Cretaceous flysch sequence (Fig. 4, Yılmaz et al., 1995). Using the TIMS Pb–Pb evaporation method, we have dated seven zircons from a sample (6821) from a banded orthogneiss. The orthogneiss is medium-grained with quartz, plagioclase, K-feldspar, hornblende, biotite, muscovite and opaque. The zircon ages range from Cambrian (516 Ma) to Mid Ordovician (464 Ma) (Fig. 7d, Table 2). As in the case of the Pamukova metagranitoid, the Ordovician age is interpreted as the age of intrusion and the older ages as mixed and/or inherited ages.

5. Discussion

The new isotopic data indicate unambiguously that the high-grade amphibolite-gneiss sequence in the Armutlu peninsula is not of Cretaceous age but forms part of the late Proterozoic–Early Palaeozoic basement of the İstanbul terrane, as initially suggested by Kaya (1977) and Yiğitbaş et al. (1999, 2004). By inference, the metaophiolite in the Almacık Massif, long regarded of Cretaceous age, must also be Precambrian in age (Yiğitbaş et al., 2004). The zircon ages from the Armutlu peninsula indicate apparently two periods of plutonism: one during the latest Proterozoic (570 Ma) and the other in Ordovician (460 Ma), with vestiges of older magmatic events at ca. 585 Ma and ca. 488 Ma. The latest Proterozoic ages are indistinguishable from those reported from the basement of the İstanbul terrane from the Bolu Massif and Karadere area (Chen et al., 2002; Ustaömer et al., 2005). However, the Mid to Late Ordovician granitoids are unknown from the İstanbul terrane *s.s.* Cambro-Ordovician granitoids have been described from the Variscan terranes in central Europe (e.g., Oliver et al., 1993; Crowley et al., 2000; von Raumer et al., 2002; Linnemann et al., 2007), where their genesis is usually ascribed to extensional events.

In the Kocaeli peninsula the Palaeozoic series start with a thick sequence of continental red sandstones and conglomerates passing up into quartz arenites, which are overlain by shallow marine sandstones, siltstones and shales that yield Early Silurian (Llandovery) paleontological ages (Fig. 3, Haas, 1968; Göncüoğlu and Sachanski, 2003). The Ordovician granitoids probably have formed part of the basement of the Kocaeli Palaeozoic series. The tectonostratigraphy of the Kocaeli Palaeozoic series suggest that the formation of the Ordovician granitoids is related to rifting of the İstanbul terrane from Gondwana with the opening of the Rheic ocean. This rifting event appears to be slightly later than that of Avalonia, which is generally considered to have rifted from Gondwana during the Early Ordovician (Arenig, 475 Ma).

In terms of age of the crystalline basement, Palaeozoic stratigraphy, palaeobiogeography and geological evolution, the İstanbul and Sakarya terranes can be compared to Avalonia and Armorican terrane assemblage, respectively, and the Intra-Pontide suture to the Rheic suture (Stampfli and Borel, 2002; Winchester and The PACE TMR Network Team, 2002). Before the Cretaceous opening of the Black Sea the İstanbul terrane was contiguous to Moesia and Scythian Platform, which exhibit similar stratigraphies. Together they formed a ribbon continent that rifted from Gondwana in the Ordovician with the opening of the Rheic ocean in its wake. The Ordovician granitoids, reported here, have possibly formed during this rifting event.

The collision of the İstanbul terrane with the Baltica is poorly constrained. The northern margin of the İstanbul terrane, where there might be stratigraphic evidence for collision lies under the Black Sea. The palaeomagnetic data from the İstanbul terrane indicate that by the Late Silurian it was part of Laurussia (Sarıbudak et al., 1989; Evans et al., 1991). The Devonian and Carboniferous foraminiferal assemblages in the İstanbul terrane are also considered typically Laurussian (Kalvoda et al., 2003). In the case of Avalonia the collision with the Baltica occurred in the latest Ordovician (Ashgill, 445 Ma, Cocks and Torsvik, 2002).

It is tempting to relate the Carboniferous deformation in the İstanbul terrane, which has characteristics of a major Palaeozoic passive continental margin, to the collision with a Sakarya arc characterized by Carboniferous granitoids and the high-temperature Carboniferous metamorphism. This would place the Sakarya terrane in an analogous position to the Armorican terrane assemblage (e.g., Torsvik and Cocks, 2004). However, the present juxtaposition of the İstanbul and Sakarya terranes does not reflect the Carboniferous tectonics. The facies boundaries in the İstanbul terrane are highly oblique to the Intra-Pontide suture suggesting rotation and removal of sections by strike-slip faulting. The presence of Cretaceous accretionary complexes along the Intra-Pontide suture zone and the absence of the Permo-Triassic Cimmeride orogenic sequences (Karakaya Complex) in the İstanbul terrane suggest Mesozoic reactivation of the Carboniferous suture. Furthermore, Tertiary strike-slip faults, including the North Anatolian Fault, have juxtaposed crustal slices, which were separated along strike (Yiğitbaş et al., 1999; Elmas and Yiğitbaş, 2001; 2005; Zattin et al., 2005; Şengör et al., 2005; Uysal et al., 2006).

6. Conclusions

The Pontides consist of terranes that were amalgamated to Baltica during the Palaeozoic in a manner analogous to the Variscan terranes in central and western Europe. In its central and eastern parts the İstanbul terrane has a Cadomian crystalline basement with late Proterozoic granitoids (ca 590–560 Ma). New isotopic data reported here show that late Proterozoic granitoids (ca 570 Ma) also occur in the western part of the İstanbul terrane and are accompanied by Ordovician (ca 460 Ma) granitoids.

Cadomian basement is not recognized in the Sakarya terrane to the south, which is characterized by Carboniferous high-temperature metamorphism and plutonism. The Sakarya terrane can be compared with the metamorphic sections of the Armorican terrane assemblage. It formed probably part of a Carboniferous arc, which collided with the İstanbul terrane or its lateral equivalents during the early Late Carboniferous. However, because of major post-Triassic tectonics, the present juxtaposition of İstanbul and Sakarya terranes does not reflect the situation during the latest Carboniferous.

Please cite this article as: Okay, A.I., et al., Defining the southern margin of Avalonia in the Pontides: Geochronological data from the Late Proterozoic and Ordovician granitoids from NW Turkey, Tectonophysics (2008), doi:10.1016/j.tecto.2008.02.004

The similarity in the evolution of the Pontide and Variscan terranes ends with the end of the Palaeozoic. In the Late Carboniferous Gondwana collided with Laurussia (Baltica, Laurentia, Avalonia, and Armorica) in the region of the central Europe thereby stabilizing the Variscan orogen. However, in the east a large ocean, the Palaeo-Tethys, continued to exist south of the Pontides (e.g., Stampfli and Borel, 2002). The Pontides were subsequently affected by the Triassic Cimmeride and latest Jurassic Balkan orogenies and by the ongoing convergence between Africa-Arabia and Eurasia plates.

Acknowledgements

This study was supported by the ITÜ-Research fund project number 31573 and by TÜBİTAK grants 101Y061 and 104Y154. Mr Adrian Wood and Ms Vanessa Pashley provided technical assistance at NERC Isotope Geosciences Laboratory. We thank Stachu Mazur and an anonymous reviewer for comments, which markedly improved the manuscript.

Appendix A. Analytical techniques

A.1. Laser ablation multicollector inductively coupled plasma mass spectrometry

Individual samples of approximately 5 kg of fresh, unaltered material were crushed and sieved using standard mineral preparation procedures. Heavy minerals were concentrated using a Wilfley table prior to settling through tetrabromoethane for separation of the heavy mineral concentrate, which was subsequently washed in acetone and dried. Zircons were separated initially by paramagnetic behaviour using a Franz isodynamic separator and then hand-picked from the non-magnetic and least magnetic fractions. The zircon separates were mounted in an araldite resin block, ground to near mid-thickness and polished.

Geochronology was determined by laser ablation multicollector inductively coupled plasma mass spectrometry (LA-MC–ICP–MS) at the NERC Isotope Geosciences Laboratory using procedures outlined by Horstwood et al. (2003). A common-Pb correction based on the measurement of ^{204}Pb was attempted, but interference from the ^{204}Hg peak overwhelmed the common-Pb contribution from the zircon grains. As a result of this, data presented is non-common Pb corrected. Analyses used a Nu Plasma MC–ICP–MS system coupled to a New Wave Research 193 nm Nd:YAG LA system. A laser spot size of 25 µm was used to ablate discrete zones within zircons. The total acquisition cycle took about one minute per ablation which equates to approximately 15 µm depth ablation pits. A ^{205}Tl/^{235}U solution was simultaneously aspirated during analysis to correct for instrumental mass bias and plasma induced inter-element fractionation using a Cetac Technologies Aridus desolvating nebulizer. Data were normalised using the zircon standard 91500 and two other zircon standards (GJ-1 and Mud Tank) were treated as unknown samples to monitor accuracy and precision of age determinations. During the analytical session GJ-1 gave a mean ^{207}Pb/^{206}Pb age of 609±20 Ma with an MSWD of 0.18 and a probability of 0.99 (reported TIMS ^{207}Pb/^{206}Pb is 608.4±0.4 Ma, F. Corfu pers comm), whereas Mud Tank gave a concordia age of 730.6±5.3 Ma MSWD 0.77, probability 0.38 (TIMS age 732±5 Ma Black & Gulson, 1978). Data were reduced and errors propagated using an in-house spreadsheet calculation package, with ages determined using the Isoplot 3 macro of Ludwig (2003).

A.2. TIMS single zircon Pb–Pb evaporation

The technique used for zircon evaporation is that developed by Kober (1986, 1987) and also described by Kröner and Todt (1988), Cocherie et al. (1992) and Klötzli (1999). ^{207}Pb/^{206}Pb zircon ages were obtained from chemically untreated zircons. Pb isotopes were measured in the mass sequence 206-207-208-204-206-207 with the Finnigan MAT 262 *TIMS* of the University of Tübingen. Pre-heating at temperatures of ca. 1350–1370 °C served as a cleaning procedure for micro-inclusions and domains with high common Pb. Temperatures of the evaporation filament for our experiments were increased in 20 °C steps during repeated evaporation steps. Only data of more than 30.000 counts/s for ^{206}Pb and with a high radiogenic Pb component (^{206}Pb/^{204}Pb > 5000) were considered for evaluation. All data were corrected for common Pb according to Cocherie et al. (1992). The common Pb corrected ^{207}Pb/^{206}Pb ratios normally define a Gaussian distribution and the mean of the ^{207}Pb/^{206}Pb ratios was derived from this distribution. ^{207}Pb/^{206}Pb ratio errors are two sigma values and refer to the last digits. For age error estimation, a 2 dimensional 1σ error (2-sigma standard deviation) of the Gaussian distribution function was applied to all measured ^{207}Pb/^{206}Pb ratios and the errors calculated according to the following formula, after Siebel et al. (2004).

$\Delta \mathrm{age} = \sqrt{\left(\left(\frac{2\sigma}{\sqrt{n}}\right)^2 + \Delta f^2\right)}$, where n is the number of ^{207}Pb/^{206}Pb isotope ratio scans, 2σ is the 2-sigma standard error of the Gaussian distribution function and Δ an assumed uncertainty of the measured ^{207}Pb/^{206}Pb ratio of 0.1%, which includes potential bias caused by mass fractionation of Pb isotopes and uncertainty in linearity of the multiplier signal. Error mean is the weighted average calculated according to Ludwig's 2003 Excel Isoplot program. The amplifiers' non-linearity was tested and found to be <0.05% in the required counting range (1–500,000 counts/s).

References

Akartuna, M., 1968. Geology of the Armutlu peninsula. Monography İstanbul Uni. Sci. Fac., 20. 105 pp. (in Turkish).

Aksay, A., Pehlivan, S., Gedik, I., Bilginer, E., Duru, M., Akbaş, B., Altun, I., 2002. Geological map of Turkey, Zonguldak sheet, scale 1:500 000. Maden Tetkik ve Arama Genel Müdürlüğü, Ankara.

Altıner, D., Koçyiğit, A., Farinacci, A., Nıcosia, U., Conti, M.A., 1991. Jurassic, Lower Cretaceous stratigraphy and paleogeographic evolution of the southern part of north-western Anatolia. Geol. Rom. 28, 13–80.

Aydın, Y., 1988. Geology of the Yıldız mountains. Selcuk Univ. Muhendis. Mimar. Fak. Derg. 2, 61–74 (in Turkish).

Black, L.P., Gulson, B.L., 1978. The age of the Mud Tank carbonatite, Strangways Range, Northern Territory. J. Aust. Geol. Geophys. 3, 227–232.

Bogdanova, S.V., Pashkevich, I.K., Gorbatschev, R., Orlyuk, M.I., 1996. Riphean rifting and major Paleoproterozoic crustal boundaries in the basement of the East European Craton: geology and geophysics. Tectonophysics 268, 1–21.

Chatalov, G., 1988. Recent developments in the geology of the Strandzha Zone in Bulgaria. Bull. Tech. Univ. Istanb. 41, 433–466.

Chen, F., Siebel, W., Satır, M., Terzioğlu, N., Saka, K., 2002. Geochronology of the Karadere basement (NW Turkey) and implications for the geological evolution of the İstanbul Zone. Int. J. Earth Sci. 91, 469–481.

Claesson, S., Bogdanova, S.V., Bibikova, E.V., Gorbatschev, R., 2001. Isotopic evidence for Palaeoproterozoic accretion in the basement of the East European Craton. Tectonophysics 339, 1–18.

Cocherie, A., Guerrot, C., Rossi, P.H., 1992. Single-zircon dating by step-wise Pb evaporation: Comparison with other geochronological techniques applied to the Hercynian granites of Corsica, France. Chem. Geol. 101, 131–141.

Cocks, L.R.M., Torsvik, T.H., 2002. Earth geography from 500 to 400 million years ago: a faunal and palaeomagnetic review. J. Geol. Soc. [Lond.] 159, 631–644.

Crowley, Q.G., Floyd, P.A., Winchester, J.A., Franke, W., Holland, J.G., 2000. Early Palaeozoic rift-related magmatism in Variscan Europe: fragmentation of the Armorican terrane assemblage. Terra Nova 12, 171–180.

Dean, W.T., Monod, O., Rickards, R.B., Demir, O., Bultynck, P., 2000. Lower Palaeozoic stratigraphy and palaeontology, Karadere–Zirze area, Pontus Mountains, northern Turkey. Geol. Mag. 137, 555–582.

Delaloye, M., Bingöl, E., 2000. Granitoids from western and northwestern Anatolia: Geochemistry and modeling of geodynamic evolution. Int. Geol. Rev. 42, 241–268.

Elmas, A., Yiğitbaş, E., 2001. Ophiolite emplacement by strike-slip tectonics between the Pontide Zone and the Sakarya Zone in northwestern Anatolia, Turkey. Int. J. Earth Sci. 90, 257–269.

Elmas, A., Yiğitbaş, E., 2005. Comment on “Tectonic evolution of the Intra-Pontide suture zone in the Armutlu Peninsula, NW Turkey” by Robertson and Ustaömer. Tectonophysics 405, 213–221.

Evans, I., Hall, S.A., Sarıbudak, M.A., Aykol, A., 1991. Preliminary palaeomagnetic results from Palaeozoic rocks of the İstanbul–Zonguldak region, N.W. Turkey. Bull. Tech. Univ. İstanb. 44, 165–190.

Franke, W., 2000. The mid-European segment of the Variscides: tectonostratigraphic units, terrane boundaries and plate tectonic evolution. In: Franke, W., Altherr, R., Haak, V., Oncken, O., Taner, D. (Eds.), Orogenic Processes: Quantification and Modelling in the Variscan Belt. Geol. Soc. London, Spec. Publ., vol. 179, pp. 35–61.

Garfunkel, Z., 2004. Origin of the Eastern Mediterranean basin: a reevaluation. Tectonophysics 391, 11–34.

Göncüoğlu, M.C., Erendil, M., 1990. Pre-Late Cretaceous tectonic units of the Armutlu Peninsula. Proceedings of the 8th Petroleum Congress of Turkey, pp. 161–168 (in Turkish).

Göncüoğlu, M.C., Sachanski, V., 2003. First findings of Upper Llandoverain (Telychian) graptolites from the Camdag area, NW Turkey. Comptes rendus de l’Academie bulgare des Sci. 56, 37–42.

Görür, N., Monod, O., Okay, A.I., Şengör, A.M.C., Tüysüz, O., Yiğitbaş, E., Sakınç, M., Akkök, R., 1997. Palaeogeographic and tectonic position of the Carboniferous rocks of the western Pontides (Turkey) in the frame of the Variscan belt. Bull. Soc. Geol. Fr. 168, 197–205.

Gradstein, F.M., Ogg, J.G., Smith, A.G., Bleeker, W., Lourens, L.J., 2004. A new geological time scale with special reference to Precambrian and Neogene. Episodes 27, 83–100.

Gutnic, M., Monod, O., Poisson, A., Dumont, J.F., 1979. Géologie des Taurides Occidentales (Turquie). Mémoires de la Sociéte Géologique de France, vol. 137, pp. 1–112.

Haas, W., 1968. Das Alt-Paläozoikum von Bithynien (Nordwest Türkei). N. Jahrb. Geol. Pal. Abh. 131, 178–242.

Horstwood, M.S.A., Foster, G.L., Parrish, R.R., Noble, S.R., Nowell, G.M., 2003. Common-Pb corrected in-situ U–Pb accessory mineral geochronology by LA-MC–ICP–MS. J. Anal. At. Spectrom. 18, 837–846.

Kalvoda, J., Leichmann, J., Babek, O., Melichar, R., 2003. Brunovistulian Terrane (Central Europe) and İstanbul Zone (NW Turkey): Late Proterozoic and Paleozoic tectonostratigraphic development and paleogeography. Geol. Carpath. 54, 139–152.

Kaya, O., 1977. Paleozoic basement structure of the Gemlik–Orhangazi region. Yerbilimleri 3, 115–128 (in Turkish).

Kaya, O., Kozur, H., 1987. A new and different Jurassic to Early Cretaceous sedimentary assemblage in northwestern Turkey (Gemlik, Bursa): implications for the pre-Jurassic to Early Cretaceous tectonic evolution. Yerbilimleri 14, 253–268.

Ketin, I., 1951. Über die Geologie der Gegend von Bayburt in Nordost-Anatolien. Istanb. UÉniv. Fen Fak. Mecm., Seri B: Tabii Ilim. 16, 113–127.

Ketin, I., 1966. Tectonic units of Anatolia. Maden Tetkik ve Arama Bull. 66, 23–34.

Klötzli, U.S., 1999. Single zircon evaporation thermal ionisation mass spectrometry: Method and procedures. Analyst 122, 1239–1248.

Kober, B., 1986. Whole grain evaporation for $^{207}Pb/^{206}Pb$ age investigations on single zircons using a double-filament thermal ion source. Contrib. Mineral. Petrol. 93, 482–490.

Kober, B., 1987. Single zircon evaporation combined with Pb^{+} emitter bedding for $^{207}Pb/^{206}Pb$-age investigations using thermal ion mass spectrometry, and implications in zirconology. Contrib. Mineral. Petrol. 96, 63–71.

Kozur, H., Göncüoğlu, M.C., 1998. Main features of the pre-Variscan development in Turkey. Acta Univ. Carol., Geol. 42, 459–464.

Kröner, A., Todt, W., 1988. Single zircon dating constraining the maximum age of the Barberton greenstone belt, southern Africa. J. Geophys. Res. 93, 15329–15337.

Linnemann, U., Gerdes, A., Drost, K., Buschmann, B., 2007. The continuum between Cadomian Orogenesis and opening of the Rheic Ocean: constraints from LA-ICP–MS U–Pb zircon dating and analysis of plate-tectonic setting (Saxo-Thuringian zone, NE Bohemian massif, Germany). In: Linnemann, U., Nance, R.D., Kraft, P., Zulauf, G. (Eds.), The Evolution of the Rheic Ocean: From Avalonian-Cadomian active margin to Alleghenian-Variscan collision. Geol. Soc. America Spec. Paper, vol. 423, pp. 61–96.

Ludwig, K.R., 2003. Isoplot 3, a geochronological toolkit for Microsoft Excel. Berkeley Geochronology Centre Special Publications, p. 1a.

Matte, P., 2001. The Variscan collage and orogeny (480–290 Ma) and the tectonic definition of the Armorican microplate: a review. Terra Nova 13, 122–128.

Nikishin, A.M., Ziegler, P.A., Stephenson, R.A., Cloetingh, S.A.P.L., Fume, A.V., Fokin, P.A., Ershov, A.V., Bolotov, S.N., Korotaev, M.V., Alekseev, A.S., Gorbachev, V.I., Shipilov, E.V., Lankreijer, A., Bembinova, E.Yu., Shalimov, I.V., 1996. Late Precambrian to Triassic history of the East European Craton dynamics of sedimentary basin evolution. Tectonophysics 268, 23–63.

Nzegge, O.M., Satir, M., 2007. Geochronology of the basement of the Central Pontides, NW Turkey: a confirmation of Eurasian origin. Geophys. Res. Abst. 9, 08626 (SRef-ID: 1607-7962/gra/EGU2007-A-08626).

Okay, A.I., Leven, E.Ja., 1996. Stratigraphy and paleontology of the Upper Paleozoic sequence in the Pulur (Bayburt) region, Eastern Pontides. Turk. J. Eart. Sci. 5, 145–155.

Okay, A.I., Monié, P., 1997. Early Mesozoic subduction in the Eastern Mediterranean: evidence from Triassic eclogite in northwest Turkey. Geology 25, 595–598.

Okay, A.I., Satır, M., Tüysüz, O., Akyüz, S., Chen, F., 2001. The tectonics of the Strandja Massif: Variscan and mid-Mesozoic deformation and metamorphism in the northern Aegean. Int. J. Earth Sci. 90, 217–233.

Okay, A.I., Monod, O., Monié, P., 2002. Triassic blueschists and eclogites from northwest Turkey: vestiges of the Paleo-Tethyan subduction. Lithos 64, 155–178.

Okay, A.I., Satır, M., Siebel, W., 2006. Pre-Alpide orogenic events in the Eastern Mediterranean region. In: Gee, D.G., Stephenson, R.A. (Eds.), European Lithosphere Dynamics. Geological Society, London, Memoirs, vol. 32, pp. 389–405.

Oliver, G.J.H., Corfu, F., Krogh, T.E., 1993. U–Pb ages from SW Poland: evidence for a Caledonian suture zone between Baltica and Gondwana. J. Geol. Soc. (Lond.) 150, 355–369.

Özgül, N., 1976. Some basic geological features of the Taurides. Türk. Jeol. Kurumu Bül. 19, 65–78 (in Turkish).

Pharaoh, T.C., 1999. Palaeozoic terranes and their lithospheric boundaries within the Trans-European Suture Zone (TESZ): a review. Tectonophysics 314, 17–41.

Robertson, A.H.F., Ustaomer, T., 2004. Tectonic evolution of the Intra-Pontide suture zone in the Armutlu Peninsula, NW Turkey. Tectonophysics 381, 175–209.

Sarıbudak, M., Sanver, M., Ponat, E., 1989. Location of western Pontides, NW Turkey, during Triassic time: preliminary palaeomagnetic results. Geophys. J. 96, 43–50.

Please cite this article as: Okay, A.I., et al., Defining the southern margin of Avalonia in the Pontides: Geochronological data from the Late Proterozoic and Ordovician granitoids from NW Turkey, Tectonophysics (2008), doi:10.1016/j.tecto.2008.02.004

Şengör, A.M.C., Yılmaz, Y., 1981. Tethyan evolution of Turkey: a plate tectonic approach. Tectonophysics 75, 181–241.

Şengör, A.M.C., Tüysüz, O., İmren, C., Sakınç, M., Eyidoğan, H., Görür, N., Le Pichon, X., Rangin, C., 2005. The North Anatolian Fault: a new look. Ann. Rev., Earth Planet. Sci. 33, 37–112.

Siebel, W., Blaha, U., Chen, F., Rohrmüller, J., 2004. Geochronology and geochemistry of a dyke-host rock association and implications for the formation of the Bavarian Pfal shear zone, Bohemian massif. Int. J. Earth Sci. 94, 8–23.

Sunal, G., Natal'in, B., Satır, M., Toraman, E., 2006. Paleozoic magmatic events in the Strandja Massif, NW Turkey. Geodin. Acta 19, 283–300.

Stampfli, G.M., 2000. Tethyan oceans In: Bozkurt, E., Winchester, J.A., Piper, J.A.D. (Eds.), Tectonics and Magmatism in Turkey and Surrounding Area. Geol. Soc. London, Spec. Publ., vol. 173, pp. 1–23.

Stampfli, G.M., Borel, G.D., 2002. A plate tectonic model for the Paleozoic and Mesozoic constrained by dynamic plate boundaries and restored synthetic oceanic isochrons. Earth Planet. Sci. Lett. 196, 17–33.

Stern, R.J., 1994. Arc assembly and continental collision in the Neoproterozoic East African Orogen. Ann. Rev. Earth Planet. Sci. 22, 319–351.

Topuz, G., Altherr, R., Kalt, A., Satır, M., Werner, O., Schwartz, W.H., 2004. Aluminous granulites from the Pulur Complex, NE Turkey: a case of partial melting, efficient melt extraction and crystallisation. Lithos 72, 183–207.

Topuz, G., Altherr, R., Schwartz, W.H., Dokuz, A., Meyer, H.-P., 2007. Variscan amphibolites-facies rocks from the Kurtoğlu metamorphic complex (Gümüşhane area, Eastern Pontides, Turkey). Int. J. Earth Sci. 96, 861–873.

Torsvik, T.H., Cocks, L.R.M., 2004. Earth geography from 400 to 250 Ma: a palaeomagnetic, faunal and facies review. J. Geol. Soc., (Lond.) 161, 555–572.

Türkecan, A., Yurtsever, A., 2002. Geological map of Turkey, Zonguldak sheet, scale 1:500 000. Maden Tetkik ve Arama Genel Müdürlüğü, Ankara.

Ustaomer, P.A., Rogers, G., 1999. The Bolu Massif: remnant of a pre-Early Ordovician active margin in the west Pontides, northern Turkey. Geol. Mag. 136, 579–592.

Ustaömer, T., Robertson, A.H.F., 2005. Reply to discussion contribution by A. Elmas and E. Yiğitbaş on "Tectonic evolution of the Intra-Pontide suture zone in the Armutlu Peninsula, NW Turkey" by A.H.F. Robertson and T. Ustaömer. Tectonophysics 405, 223–231.

Ustaömer, P.A., Mundil, R., Renne, P.R., 2005. U/Pb and Pb/Pb zircon ages for arc-related intrusions of the Bolu Massif (W Pontides, NW Turkey): evidence for Late Precambrian (Cadomian) age. Terra Nova 17, 215–223.

Uysal, I.T., Mutlu, H., Altunel, E., Karabacak, V., Golding, S.D., 2006. Clay mineralogical and isotopic (K–Ar, δ18O, δD) constraints on the evolution of the North Anatolian Fault Zone, Turkey. Earth Planet. Sci. Lett. 243, 181–194.

von Raumer, J.F., Stampfli, G.M., Borel, G., Bussy, F., 2002. Organization of pre-Variscan basement areas at the north-Gondwanan margin. Int. J. Earth Sci. 91, 35–52.

Winchester, J.A., The PACE TMR Network Team, 2002. Palaeozoic amalgamation of Central Europe: new results from recent geological and geophysical investigations. Tectonophysics 360, 5–21.

Yiğitbaş, E., Elmas, A., Yılmaz, Y., 1999. Pre-Cenozoic tectono-stratigraphic components of the western Pontides and their geological evolution. Geol. J. 34, 55–74.

Yiğitbaş, E., Kerrich, R., Yılmaz, Y., Elmas, A., Xie, Q.L., 2004. Characteristics and geochemistry of Precambrian ophiolites and related volcanics from the İstanbul–Zonguldak Unit, Northwestern Anatolia, Turkey: following the missing chain of the Precambrian South European suture zone to the east. Precambrian Res. 132, 179–206.

Yılmaz, I., 1977. The absolute age and genesis of the Sancaktepe granite (Kocaeli peninsula)]. Türk. Jeol. Kurumu Bül. 20, 17–20 (in Turkish).

Yılmaz, Y., 1990. Allochthonous terranes in the Tethyan Middle East, Anatolia and surrounding regions. Phil. Trans. Roy. Soc., Lond. A 331, 611–624.

Yılmaz, Y., Tüysüz, O., Gözübol, A.M., Yiğitbaş, E., 1981. Geological evolution of the tectonic units lying south and north of the North Anatolian Fault Zone between Abant (Bolu) and Dokurcun (Sakarya). Istanb. Yerbilim. Derg. 2, 239–261 (in Turkish).

Yılmaz, Y., Genç, S.C., Yigitbaş, E., Bozcu, M., Yılmaz, K., 1995. Geological evolution of the late Mesozoic continental margin, Northwestern Anatolia. Tectonophysics 243, 155–171.

Zapcı, C., Akyüz, H.S., Sunal, G., 2003. An approach to the structural evolution of the İstanbul Zone. Proceeding of the Symposium on the Geology of the İstanbul Region, İstanbul, pp. 5–14 (in Turkish).

Zattin, M., Okay, A.I., Cavazza, W., 2005. Fission-track evidence for late Oligocene and mid-Miocene activity along the North Anatolian Fault in southwestern Thrace. Terra Nova 17, 95–101.